

Finally we would like to emphasize that double layers have never been observed in one-dimensional simulations on a very long system. This is in sharp contrast to the ion-acoustic-instability simulations, where double layers were almost always found.⁸ It appears that hydrogen cyclotron waves observed along auroral field lines may be an effect of double layers rather than a cause for generating them.³

It is a pleasure to thank Dr. M. Ashour-Abdalla, Dr. J. M. Dawson, Dr. C. T. Dum, Dr. F. W. Perkins, Dr. T. Sato, and, in particular, Dr. M. Yamada for their interest and encouragement.

This work was supported by the United States Department of Energy Contract No. DE-ACOZ-76-CH03073.

¹W. E. Drummond and M. N. Rosenbluth, *Phys. Fluids*

5, 1507 (1962).

²TFR Group, *Phys. Rev. Lett.* **41**, 113 (1978).

³F. S. Mozer, C. W. Carlson, M. K. Hudson, R. B. Torbert, B. Paraday, J. Yatteau, and M. C. Kelley, *Phys. Rev. Lett.* **38**, 292 (1977).

⁴M. Yamada and H. W. Hendel, *Phys. Fluids* **21**, 1555 (1978).

⁵H. Bohmer and S. Fornaca, *J. Geophys. Res.* **84**, 5234 (1979).

⁶W. W. Lee and H. Okuda, *J. Comput. Phys.* **26**, 139 (1978).

⁷C. T. Dum and T. H. Dupree, *Phys. Fluids* **13**, 2064 (1970).

⁸T. Sato and H. Okuda, *Phys. Rev. Lett.* **44**, 740 (1980), and Plasma Physics Laboratory Report No. PPPL-1681 (to be published).

⁹B. B. Kadomtsev, *Plasma Turbulence* (Academic, New York, 1965), p. 84.

¹⁰M. Yamada, H. W. Hendel, S. Seiler, and S. Ichimaru, *Phys. Rev. Lett.* **34**, 650 (1975).

¹¹S. Seiler and M. Yamada, *Nucl. Fusion* **19**, 469 (1979).

Electron Heating and Confinement Measurements in the EBT-S Toroidal Core Plasma with Thomson Scattering

L. Bighel and J. A. Cobble

Oak Ridge National Laboratory, Oak Ridge, Tennessee 37830

(Received 25 August 1980)

A ruby-laser Thomson-scattering system, designed for very low-electron-density applications, has shown electron temperature (T_e) and density (n_e) profiles in the Elmo Bumpy Torus-Scale toroidal plasma to be flat, with T_e values from 50 to 500 eV and n_e values from 0.5 to 2.2×10^{12} cm⁻³. Scaling of T_e and n_e with microwave power and background pressure is discussed. Electron-energy confinement times are derived and are found to scale approximately linearly with power for times up to 4 ms.

PACS numbers: 52.25.Lp, 52.50.Jm, 52.70.Kz

Elmo Bumpy Torus-Scale (EBT-S), the successor to EBT-I,¹ is a steady-state, microwave-heated toroidal plasma device consisting of 24 mirror sections with a mirror ratio of 2, a major radius of 150 cm, and a minor radius of 11 cm in the mirror coil throats. Reported here for the first time are the results of detailed electron-confinement studies on this, the second in the series of machines now designated by the U. S. Department of Energy as the leading alternative concept to tokamaks and mirrors for magnetically confined fusion. The method of investigation used was ruby-laser Thomson scattering, which at the 10^{12} -cm⁻³ electron density of EBT-S is an exacting task.² Radial profile data are presented and empirical scalings of plasma parameters are dis-

cussed.

The plasma was continuously maintained by electron-cyclotron-resonance heating with up to 60 kW of 28-GHz power supplied by a gyrotron.³ Of this, approximately 5–10 kW reached the toroidal core plasma, as is shown later. In each of the 24 sections, fundamental resonance regions are located about midway between the mirror coil throats and the midplane between them. There is also an annular, second-harmonic resonance region near the minor circumference of the core in the midplane. A 500-keV population of precessing electrons, the so-called hot-electron ring,⁴ is produced in the annular region. Supplementary ring profile heating at 18 GHz is also used.

The scattering system employs a 14-J ruby la-

ser and a polychromator with a Rayleigh-calibration channel and five channels from 700 to 740 nm for Thomson data. A rotatable mirror, which preserves the conjugate focal planes of a stationary lens system, enables the radial scans. The scans were limited to a region extending from the plasma center outward 8 cm. A complete scan contains 20–25 laser shots, each of which yields T_e and n_e data. The usual spectrum includes a total of 20–30 counted photons in all the five channels. This is the expected level at the relatively low density of the experiment. Most spectra (about 40% of all shots and 65% of those free of plasma light) consist of three to five points to which can be fitted Gaussian curves with correlation coefficients ≥ 0.95 .

Figure 1 shows radial scans of T_e and n_e with

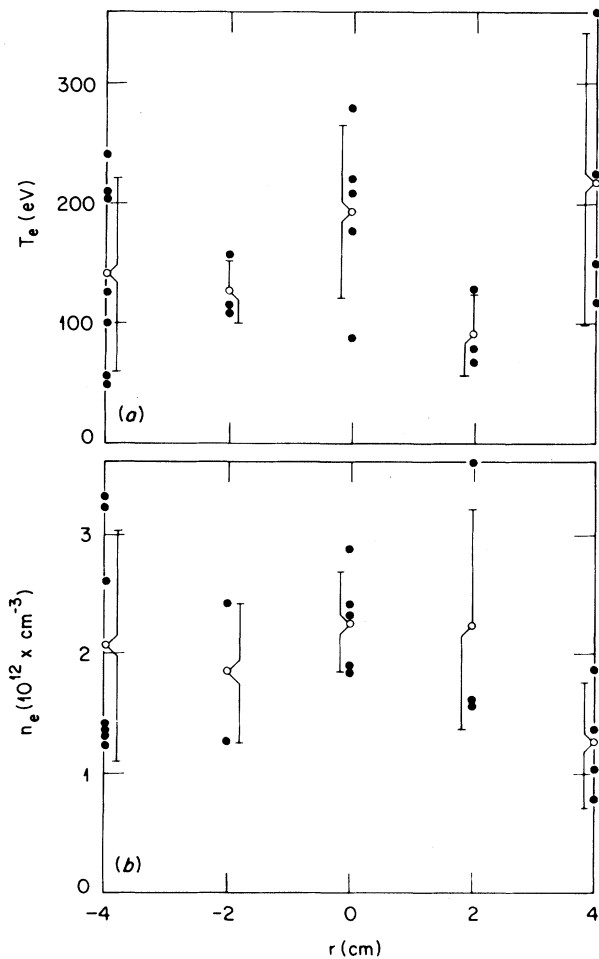


FIG. 1. Radial profiles of (a) T_e and (b) n_e with $P_{28} = 54$ kW, $P_{18} = 10$ kW, and 4×10^{-6} Torr of hydrogen ($r = 0$ is the geometric center; $r = -4$ is the plasma center).

average values and standard deviations for a 54-kW gyrotron run of nearly an hour. During the run, pressure was held constant as was the 18-GHz profile heating power of 10 kW. Although there is considerable spread in the data, the profiles for all microwave powers are reasonably flat within the large error bars.

The two EBT-S parameters that are easily adjustable externally are hydrogen background pressure and microwave power. Experimental scaling of T_e and n_e with pressure involves keeping constant the gyrotron power and staying in the low-fluctuation T mode (toroidal mode). Scaling with microwave power was carried out at constant pressure (at the low-pressure end of the T mode) and was limited only by concern for overheating of the gyrotron employed.

In what follows, the values of T_e and n_e averaged over the 8-cm profiles are used to derive empirical scaling laws of these variables versus gyrotron power. Figure 2 shows how T_e increases approximately as $P_{\mu}^{1.5}$, where P_{μ} is the gyrotron power output. This dependence is in agreement with previous though less complete data ob-

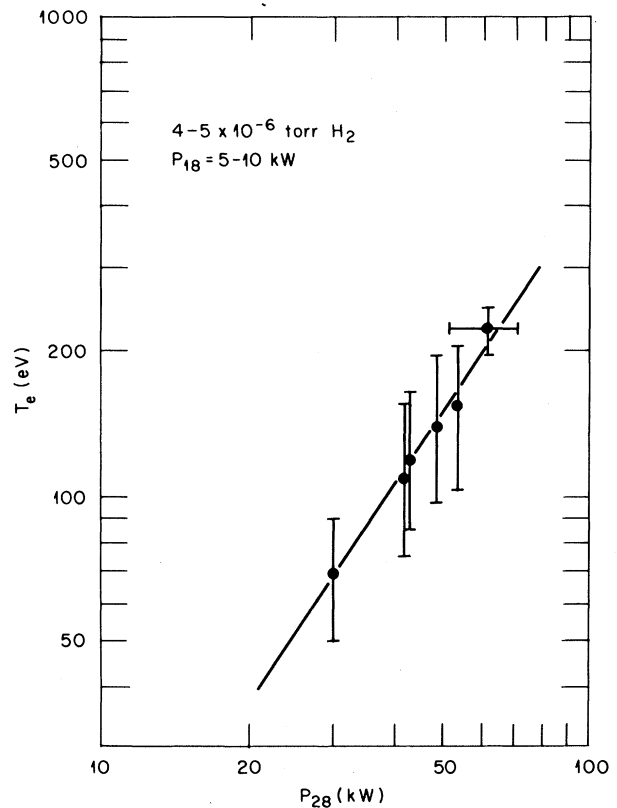


FIG. 2. T_e as a function of total 28-GHz gyrotron power output.

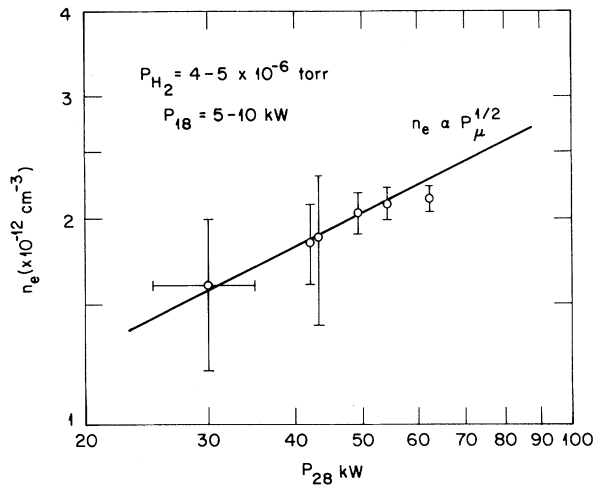


FIG. 3. n_e as a function of total 28-GHz gyrotron power output.

tained with a different gyrotron and microwave distribution system.² A systematic difference between the two sets of data (the former showed higher temperatures) can now be explained only qualitatively in terms of the differences in microwave coupling of the two systems.

The behavior of n_e (radially averaged over the 8-cm range) with microwave power at constant pressure is shown in Fig. 3. The electron density increases approximately as $P_\mu^{0.5}$ over the available range of microwave power.

Figure 4 shows T_e and n_e as functions of background pressure for 30 kW of 28-GHz power. The scattering measurements in this case were all taken at a single position near the plasma center ($r = -4$ cm). The values of T_e and n_e used for scaling with pressure are averages of up to three spectra for each pressure setting. The central electron temperature increases with decreasing pressure as predicted by theory.⁵ The temperature rises from about 50 eV at 2×10^{-5} Torr to 150 eV at 3×10^{-6} Torr. The central electron density exhibits a broad plateau at $(1.3 \pm 0.2) \times 10^{12}$ cm⁻³ between 5 and 15×10^{-6} Torr. At pressures below and above this range there are indications of a fall in n_e .

The core electron-energy confinement time can be defined as

$$\tau_{Ee} = (1/P_{\mu c}) \int \frac{3}{2} n_e T_e dV, \quad (1)$$

where $P_{\mu c}$ is the steady-state microwave power that heats the core electrons. The laser measurements of T_e and n_e provide radial profile infor-

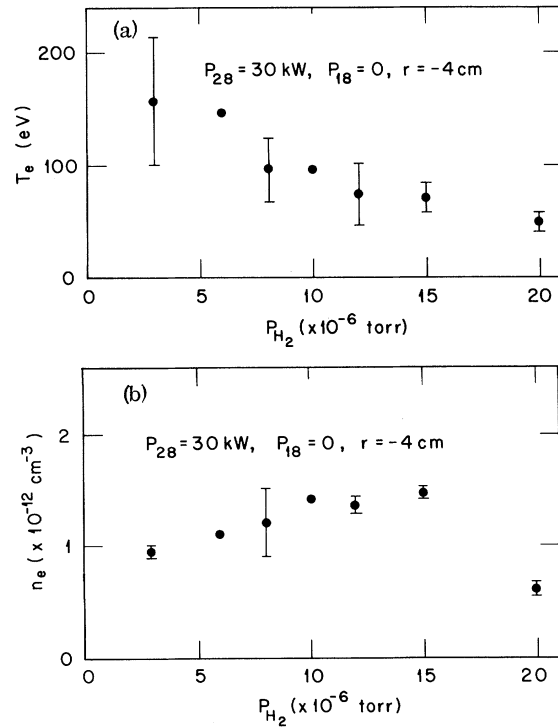


FIG. 4. The dependence on background pressure of (a) T_e and (b) n_e measured at the plasma center for 30-kW gyrotron power output.

mation over 8 cm outward from the plasma center. If we assume azimuthal symmetry, the volume-integrated core electron energy can be estimated. The microwave power that heats the core can be expressed as⁶

$$P_{\mu c} = (a_c/a_r)^2 (\eta P_\mu - N P_r), \quad (2)$$

where η is the efficiency of microwave transmission, N is the number of hot electron annuli (≤ 24), P_r is the microwave power absorbed by each annulus, a_c is the core radius in the fundamental resonance region, and a_r is the radius of the fundamental resonance region.

The values of P_μ and η are determined calorimetrically. The values of a_c and a_r are calculated from the magnetic field geometry and from toroidally passing particle-orbit considerations. The ring power input is determined by the ring analog of Eq. (1). The ring temperature and density are measured with hard-x-ray spectroscopy,⁴ and the ring volume is estimated with skimmer probes. The ring energy confinement time is measured by monitoring the decay of the ring diamagnetic signal and also of the synchrotron emission from the ring.

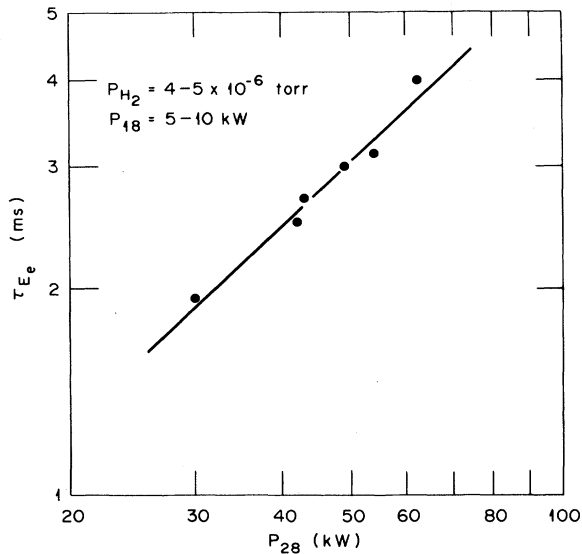


FIG. 5. Electron-energy-confinement time as a function of total 28-GHz gyrotron power output.

For the measurements described here, the fraction of the total gyrotron power that heats the core, thus estimated, is 10% to 15%. In Fig. 5, τ_{Ee} is shown as a function of P_{μ} for T -mode operation assuming 12% coupling to the core and neglecting profile heating. The uncertainties in the values of τ_{Ee} (not shown on the graph) are compounded from the uncertainties in the two-dimensional profiles, the average core radius, the estimate of $P_{\mu c}$, and the neglect of core heating by the rings. Notwithstanding the large level of uncertainty, τ_{Ee} shows a reasonably linear dependence on P_{μ} , with values ranging from 2 ms at 30 kW to 4 ms at 60 kW.

In conclusion, Thomson-scattering measurements have shown flat T_e and n_e profiles for a wide range of conditions in EBT-S. T_e was found

to increase with decreasing pressure in the T mode at constant microwave power input, while n_e remained fairly constant with pressure. Empirical scalings of electron parameters with microwave power input at constant pressure (at the low-pressure end of the T mode), and for a particular gyrotron and microwave transmission system, indicate $T_e \propto P_{\mu}^{1.5}$, $n_e \propto P_{\mu}^{0.5}$, and $\tau_{Ee} \propto P_{\mu}$. A considerable theoretical and experimental effort is currently aimed at understanding the observed scalings, while increasing the range of the radial scans and extending the scalings to higher power levels.

The authors acknowledge the direction of John Sheffield and the cooperation of the entire staff of EBT-S.

This work was sponsored by the Office of Fusion Energy, U. S. Department of Energy under Contract No. W-7405-eng-26 with the Union Carbide Corporation.

¹R. A. Dandl *et al.*, ORNL Report No. ORNL/TM-6457, 1978 (unpublished).

²L. Bighel and J. A. Cobble, ORNL Report No. ORNL/TM-7437, 1980 (unpublished).

³H. Jory *et al.*, in Proceedings of the Fourth International Conference on Infrared and Millimeter Waves and Their Applications, Miami Beach, Florida, December, 1979, edited by S. Terkowitz (unpublished), p. 158.

⁴N. Uckan *et al.*, in Proceedings of the Eighth International Conference on Plasma Physics and Controlled Nuclear Fusion Research, Brussels, Belgium, July, 1980 (to be published).

⁵E. F. Jaeger, C. L. Hedrick, and D. A. Spong, Nucl. Fusion **19**, 1627 (1979).

⁶D. B. Batchelor, ORNL Report No. ORNL/TM-7001 (unpublished).